

Accepted Manuscript

Research paper

Synthesis, characterization and antimicrobial studies of organotin(IV) complexes of *N*-methyl-*N*-phenyldithiocarbamate

Jerry O. Adeyemi, Damian C. Onwudiwe, Anthony C. Ekennia, Chinonso R. Uwaoma, Eric C. Hosten

PII: S0020-1693(17)31875-3
DOI: <https://doi.org/10.1016/j.ica.2018.02.034>
Reference: ICA 18144

To appear in: *Inorganica Chimica Acta*

Received Date: 12 December 2017
Revised Date: 26 February 2018
Accepted Date: 27 February 2018



Please cite this article as: J.O. Adeyemi, D.C. Onwudiwe, A.C. Ekennia, C.R. Uwaoma, E.C. Hosten, Synthesis, characterization and antimicrobial studies of organotin(IV) complexes of *N*-methyl-*N*-phenyldithiocarbamate, *Inorganica Chimica Acta* (2018), doi: <https://doi.org/10.1016/j.ica.2018.02.034>

This is a PDF file of an unedited manuscript that has been accepted for publication. As a service to our customers we are providing this early version of the manuscript. The manuscript will undergo copyediting, typesetting, and review of the resulting proof before it is published in its final form. Please note that during the production process errors may be discovered which could affect the content, and all legal disclaimers that apply to the journal pertain.

Synthesis, characterization and antimicrobial studies of organotin(IV) complexes of *N*-methyl-*N*-phenyldithiocarbamate

^{1,2}Jerry O. Adeyemi, ^{1,2}Damian C. Onwudiwe*, ³Anthony C. Ekennia, ⁴Chinonso R. Uwaoma, ⁵Eric C. Hosten

¹Material Science Innovation and Modelling (MaSIM) Research Focus Area, Faculty of Natural and Agriculture Science, North-West University (Mafikeng Campus), Private Bag X2046, Mmabatho, South-Africa.

²Department of Chemistry, School of Chemical and Physical Sciences, Faculty of Natural and Agriculture Science, North-West University (Mafikeng Campus), Private Bag X2046, Mmabatho 2735, South Africa.

³Department of Chemistry, Federal University Ndufu-Alike Ikwo, PMB 1010, Abakaliki, Ebonyi State, Nigeria.

⁴Chemical Resource Beneficiation, North-West University, Potchefstroom Campus, P O Box X6001, Potchefstroom, 2520, South Africa.

⁵Department of Chemistry, Nelson Mandela University, P.O Box 77000, Port Elizabeth 6031, South Africa.

* Corresponding author

Email: Damian.Onwudiwe@nwu.ac.za

Tel: +27 18 389 2545

Fax: +27 18 389-2420

ABSTRACT

Organotin(IV) dithiocarbamate complexes have shown a large spectrum of biological activities, which includes antioxidants, anti-inflammatory, antimicrobial, antituberculosis, anticancer and antiviral. In this report, organotin(IV) dithiocarbamate complexes derived from *N*-methyl-*N*-phenyldithiocarbamate (L) and organotin have been synthesized. The complexes which were represented as $C_4H_9(Cl)SnL_2$ (1), $C_6H_5(Cl)SnL_2$ (2), $(CH_3)_2SnL_2$ (3), $(C_4H_9)_2SnL_2$ (4) and $(C_6H_5)_2SnL_2$ (5), were characterized by spectroscopic techniques (FTIR, 1H , ^{13}C and ^{119}Sn NMR), elemental and thermal analyses (TGA and DTG). The structures of complexes (3) and (4) were further established by X-ray single crystal diffraction. The structures, in both complexes, gave a distorted octahedral geometry around the tin center. This is due to the longer distance of one of the Sn-S bonds within the complexes compared to others, and also the electronic and steric demands caused by the alkyl substituents on the tin atom. The complexes exhibited varied antimicrobial activity against *S. Aureus*, *B. cerues*, *K. pneumonia*, *P. aeruginosa*, *E. coli*, *C. albican* and *A. flavus*. Complex 5 displayed the best antimicrobial activities compared to the other organotin complexes, and this could be attributed to the planar phenyl group attached to the tin center causing an increase in the lipophilicity of the complex through the lipid bilayer of the bacteria organisms.

Keywords: Organotin(IV); antimicrobial; dithiocarbamate; thermal studies

1. INTRODUCTION

Organotin(IV) complexes possess at least one covalent carbon to organotin bond as part of its structural characteristics [1]. It also contains tin in a +4 oxidation state bonded to donor atoms of a number of ligands. They have received a lot of research interests due to their structural diversity and numerous applications [2]. A series of tri-alkyl/acyl-substituted-organotin(IV) complexes: tri-n-butylorganotin, tricyclohexylorganotin, and triphenylorganotin compounds are used as biocides for agricultural and industrial applications; and as antifouling agents and disinfectants for surface materials [3]. Similarly, triorganotin(IV) complexes are used as catalysts in some synthetic reactions like the production of polyurethanes [4].

Compounds containing organotin(IV) moieties display biological potentials which has been utilized in their applications as important pharmacophore in the development of metal based drugs [5]. Organotin(IV) derivatives have been reported to exhibit antimicrobial [6], anti-inflammatory [7], cardiovascular [8], trypanocidal [9], antiherpes [10] and antituberculosis activities [11]. However, the activity of the organotin(IV) derivatives is a function of the nature (chemical and biological properties) of the organic ligands (containing hetero donor atoms such as O, N, S) bonded to a particular organotin(IV) moiety [12]. Therefore attention have been directed toward organic ligands of chemotherapeutic importance such as amino acids, Schiff bases, peptides, carbohydrates, dithiocarbamates as coordinating ligands for several organotin(IV) compounds [13].

Dithiocarbamate ligands are important in coordination and solid state chemistry due to their ability to stabilize metal ions of different oxidation states [14]. This property is attributed to the different resonance forms and the delocalization of the nitrogen lone pair onto the sulfur atoms of the dithiocarbamate moiety. The high nucleophilic property of the ligands towards various

metal ions has led to the existence of a large catalogue of dithiocarbamate complexes [15]. Dithiocarbamates have been reported to show antimicrobial [16], anti-inflammatory [17], antioxidant [18], and anticancer [19] properties. Furthermore, organotin(IV) complexes containing dithiocarbamate molecules have been shown to possess enhanced biological properties [20–22]. In the light of the potentials of dithiocarbamate based ligands, we report here the synthesis, characterization and thermal analyses of a series of new complexes of organotin(IV) complexes of *N*-methyl-*N*-phenyldithiocarbamate. The antimicrobial potentials of the organotin complexes were examined using Agar well diffusion method against two fungi and five Gram (+) and Gram (-) bacteria.

2. Experimental

2.1 Materials and methods

All reagents and solvents were of analytical grade. They were obtained from Merck/Sigma–Aldrich and were used as received. Elemental (CHNS) analysis was carried out using Elementar Vario EL Cube. Infrared spectra were obtained using Alpha Bruker FTIR spectrometer (frequency range 4000 – 400 cm^{-1}). Nuclear magnetic resonance (^1H and ^{13}C) spectra were obtained using Bruker Avance III 600 MHz NMR spectrometer. CDCl_3 was used as a solvent and tetramethylsilane as internal standard, while the ^{119}Sn was measured on a Bruker Ascend 500MHz Avance III HD equipped with BBO Probe. In the ^{119}Sn NMR, the chemical shifts were measured with reference to $(\text{CH}_3)_4\text{Sn}$ as an external standard. The multiplicities of the signals in the ^1H NMR, are given with chemical shifts, (s = singlet, d = doublet, t = triplet, q = quartet, m= multiplet). Thermogravimetric (TG/DTG) analysis was performed on SDTQ 600 thermal

instrument. Samples were heated at the rate of $10\text{ }^{\circ}\text{C min}^{-1}$ in alumina crucibles under flowing nitrogen.

2.2 Synthesis of ammonium *N*-methyl-*N*-phenyldithiocarbamate (L)

Ammonium *N*-methyl-*N*-phenyldithiocarbamate (L) was prepared following a similar procedure described previously [23]. *N*-methyl aniline (1.08 mL, 0.01 mol) was introduced into a round bottom flask in an ice bath at approximately $2\text{ }^{\circ}\text{C}$, followed by the addition of ammonia solution (3 mL, 0.01 mol) with continuous stirring for 5 min. Then, carbon disulfide (0.60 mL, 0.01 mol) was added dropwise to the mixture and stirred for 5 h. A faint yellowish product precipitated out of the mixture, and collected by filtration.

2.3 Synthesis of the organotin(IV) complexes, R_2SnCl_2 and R_2SnL_2 (R = CH_3 , C_4H_9 , C_6H_5)

About 20 mL ethanol solution of the respective organotin(IV) chloride (R_2SnCl_2 and R_2SnCl_2) was reacted with 20 mL ethanol solution of the ligand in 1: 2 mole ratio (organotin:ligand) in ice for 2 h. The resultant white precipitates were filtered, washed with ethanol and dried under vacuum.

(1) $(\text{C}_4\text{H}_9)\text{ClSnL}_2$: Yield: 2.75 g (78.0%); M.Pt: $190 - 192\text{ }^{\circ}\text{C}$; Selected FTIR, ν (cm^{-1}): 1490 (C-N), 971, 962 (C=S), 2955(aliphatic C-H), 3048 (aromatic C-H), 552 (Sn-C), 403 (Sn-S); ^1H NMR (CDCl_3): δ ppm = 7.39 - 7.19 (m, 10H, N- C_6H_5), 3.67 (s, 6H, N- CH_3), 0.97 (t, 3H, $\text{CH}_2\text{CH}_2\text{CH}_2\text{CH}_3$), 1.43 (m, 2H, $\text{CH}_2\text{CH}_2\text{CH}_2\text{CH}_3$), 1.99 (m, 2H, $\text{CH}_2\text{CH}_2\text{CH}_2\text{CH}_3$), 2.38 (t, 2H, $\text{CH}_2\text{CH}_2\text{CH}_2\text{CH}_3$); ^{13}C NMR (CDCl_3) δ ppm = 147.3, 129.4, 128.1, 125.8 ($-\text{C}_6\text{H}_5$), 47.4 (N- CH_3), 205.3($-\text{CS}_2$), 13.9 ($\text{CH}_2\text{CH}_2\text{CH}_2\text{CH}_3$), 25.3 ($\text{CH}_2\text{CH}_2\text{CH}_2\text{CH}_3$), 29.3 ($\text{CH}_2\text{CH}_2\text{CH}_2\text{CH}_3$), 30.9 ($\text{CH}_2\text{CH}_2\text{CH}_2\text{CH}_3$); ^{119}Sn NMR (CDCl_3): δ ppm = -204.40; Anal. Calcd (%) for

$C_{20}H_{25}ClN_2S_4Sn$ (575.96): C, 41.71; H, 4.38; N, 4.86; S, 22.27. Found: C, 40.91; H, 4.08; N, 4.99; S, 22.57.

(2) $(C_6H_5)ClSnL_2$: Yield: 3.10 g (84%); M.Pt. 179 -181 °C; Selected FTIR, ν (cm^{-1}): 1491 (C-N), 1002, 996 (C=S), 2806 (aliphatic C-H), 3039 (aromatic C-H), 553 (Sn-C), 448 (Sn-S); 1H NMR ($CDCl_3$) δ ppm = 7.40 - 7.12 (m, 10H, $-C_6H_5$), 3.52 (s, 6H, $N-CH_3$), 7.99 - 7.56 (m, 5, Sn- C_6H_5); ^{13}C NMR ($CDCl_3$) δ = 142.34, 135.09, 129.11, 128.07 (N- C_6H_5), 50.01 ($-CH_3$), 200.03 ($-CS_2$), 135.09- 122.12 (Sn- C_6H_5) ppm; ^{119}Sn NMR ($CDCl_3$): δ ppm = -286.57; Anal. Calcd (%) for $C_{22}H_{21}ClN_2S_4Sn$ (595.93): C, 44.35; H, 3.55; N, 4.70; S, 21.53 Found: C, 43.95; H, 4.01; N, 4.91; S, 22.03. .

(3) $(CH_3)_2SnL_2$: Single crystal for x-ray analysis was obtained in dichloromethane-ethanol 3:1. Yield: 2.79 g (85%); M.Pt 121 – 122 °C; Selected FTIR, ν (cm^{-1}): 1488 (C-N), 1002 (C=S), 2912 (aliphatic C-H), 3005 (aromatic C-H), 555 (Sn-C), 420 (Sn-S); 1H NMR ($CDCl_3$) δ ppm = 7.31 - 7.22 (m, 10H, N- C_6H_5), 3.67 (s, 6H, $N-CH_3$), 1.51 (s, 6H, Sn- CH_3); ^{13}C NMR ($CDCl_3$) δ ppm = 146.70, 129.49, 128.30, 125.95 ($-C_6H_5$), 46.49($N-CH_3$), 202.82($-CS_2$), 14.04 (Sn- CH_3); ^{119}Sn NMR ($CDCl_3$): δ ppm = -312.93; Anal. Calcd (%) for $C_{18}H_{22}N_2S_4Sn$ (513.97): C, 42.11; H, 4.32; N, 5.46; S, 24.98. Found: C, 41.21; H, 4.92; N, 5.56; S, 23.48.

(4) $(C_4H_9)_2SnL_2$: Single crystal for x-ray analysis was obtained in dichloromethane-ethanol 4:1. Yield: 2.70 g (73%); M.Pt. 130 – 132 °C; Selected FTIR, ν (cm^{-1}): 1489 (C-N), 963 (C=S), 2914 (aliphatic C-H), 3036 (aromatic C-H), 554 (Sn-C), 407 (Sn-S); 1H NMR ($CDCl_3$) δ ppm = 7.39 - 7.19 (m, 10, N- C_6H_5), 3.68 (s, 6H, $N-CH_3$), 0.95 (t, 6H, $CH_2CH_2CH_2CH_3$), 1.46 (m, 4H, $CH_2CH_2CH_2CH_3$), 1.93 (m, 4H, $CH_2CH_2CH_2CH_3$), 2.04 (t, 4H, $CH_2CH_2CH_2CH_3$); ^{13}C NMR

(CDCl₃) δ ppm = 146.91, 129.46, 128.18, 126.01 (N-C₆H₅), 46.46 (N-CH₃), 203.80 (-CS₂), 13.86 (CH₂CH₂CH₂CH₃), 26.49 (CH₂CH₂CH₂CH₃), 28.66 (CH₂CH₂CH₂CH₃), 33.39 (CH₂CH₂CH₂CH₃); ¹¹⁹Sn NMR (CDCl₃): δ ppm = -268.07; Anal. Calcd (%) for C₂₄H₃₄N₂S₄Sn (598.1): C, 48.25; H, 5.74; N, 4.69; S, 21.46. Found: C, 48.15; H, 5.66; N, 4.21; S, 20.96.

(5) (C₆H₅)₂SnL₂: Yield: 2.65 g (68%), M.Pt; 183 – 185 °C; Selected FTIR, ν (cm⁻¹): 1482 (C-N), 996 (C=S), 2987 (aliphatic C-H), 3055 (aromatic C-H), 553 (Sn-C), 418 (Sn-S); ¹H NMR (CDCl₃) δ ppm = 7.42 - 7.11 (m, 10H, N-C₆H₅), 7.98-7.72(m, 10H, Sn-C₆H₅), 3.59 (s, 6H, N-CH₃); ¹³C NMR (CDCl₃) δ ppm = 146.97, 129.50, 128.64, 125.76 (N-C₆H₅), 47.29 (N-CH₃), 201.94 (-CS₂), 135.80 - 128.33, (Sn-C₆H₅); ¹¹⁹Sn NMR (CDCl₃): δ ppm = -312.04 ; Anal. Calcd (%) for C₂₈H₂₆N₂S₄Sn (638.0): C, 52.76; H, 4.11; N, 4.39; S, 20.12. Found: C, 51.96; H, 3.98; N, 4.01; S, 21.01.

2.4 X-ray crystallography

Single crystals of complexes 3 and 4 were diffracted using a Bruker Kappa Apex II diffractometer with monochromated Mo K α radiation (λ = 0.71073 Å) at 200 K. APEX2 and SAINT was used for data collection and cell refinement [24]. SHELXT-2014 and SHELXL-2016 were used for resolving and refining, respectively, by least square procedures [25, 26]. SHELXLE was used as a graphical interface [27]. Data correction of absorption effect was achieved by a numerical method using SADABS [24]. H atom bonded to carbon were placed in calculated points and incorporated in the refinement in the riding model approximation with $U_{\text{iso}}(\text{H})$ set to $1.2U_{\text{eq}}(\text{C})$. To best fit the experimental density (HFIX 137 in the SHELX program suite (Sheldrick, 2015)), with $U_{\text{iso}}(\text{H})$ set to $1.5U_{\text{eq}}(\text{C})$, H atoms of the methyl moiety were allowed to rotate with a fixed angle around C---C bonds.

2.5 Antimicrobial studies

Clinical isolates of different microbial strains were collected from department of Microbiology, Federal Teaching Hospital, Abakaliki, Nigeria. The bacteria strains were Gram negative (*Escherichia coli*, *Klebsiella Pneumonia* and *Pseudomonas Aeruginosa*) and Gram positive (*Bacillus cereus* and *Staphylococcus aureus*) organisms. The fungi are *Candida albicans* and *Aspergillus flavus*. The microbial strains were selected based on their clinical and pharmacological relevance [28]. Antimicrobial screening was carried out using agar disc diffusion method [29] at the Department of Microbiology, Federal University Ndufu Alike Ikwo, and Nigeria.

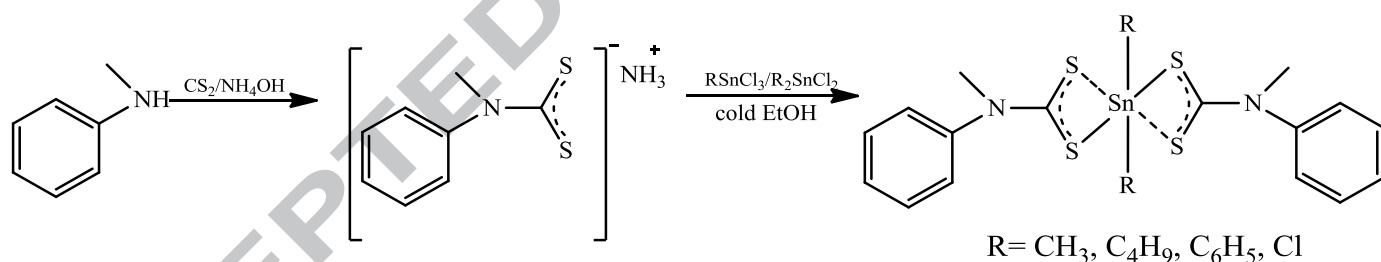
The petri plates were prepared using sterile Muller–Hinton agar (MHA). The inoculum of test cultures (10^6 CFU/mL) were streaked onto the condensed Muller Hinton agar in petri plates using a sterilized cotton swab, in order to ensure a uniform thick lawn or layer of growth, and allowed to dry for 15 min. About 10, 25 and 50 $\mu\text{g/mL}$ concentrations of stock solutions of the complexes were prepared using 80% dimethylsulfoxide (DMSO) as diluent [30, 31]. Consequently, wells were bored into the solidified agar surfaces on the petri dishes using 6 mm sterile cork borer and were impregnated with 25 μL of the sample stock solutions. About 20 μL of 1.25 mg/mL 3-(4, 5-dimethylthiazol-2-yl)-2, 5-diphenyltetrazolium bromide (MTT) (Sigma-Aldrich) was added to each plate and observed for a purple colouration [31]. The plates were incubated for 24 h at 37 °C for the bacteria and 48 h at 30 °C for the fungi strains. Control experiments were carried out under similar condition by using commercially available antibacterial drug (Sulfamethoxazole) and an antifungal drug (Ketoconazole) as the positive control drugs, while 80% dimethylsulfoxide was used as a negative control. The sensitivities of the microorganism species to the samples were determined by measuring the sizes of inhibitory

zones (including the diameter of disk) on the agar surface around the disks, and values <6 mm were considered as inactive against the microorganisms. Zones of inhibition were recorded in millimetres and the experiment was repeated in quadruplet. Experimental results were given as mean \pm S.D. of the four parallel measurements.

3. Results and discussion

3.1 Synthesis

The ammonium salt of the dithiocarbamate ligand was prepared using a one pot reaction system and was obtained in good yield. The synthesis of the respective metal complexes of the ligand were achieved by the reaction of the respective organotin(IV) chloride ($R\text{SnCl}_3$ and $R_2\text{SnCl}_2$) salts with the ligand (L) according to Scheme 1. The reaction proceeded by the displacement of the chloride ions of the organotin(IV) salts by the ligand (L).^q



Scheme 1: synthesis of *N*-methyl-*N*-phenyl dithiocarbamate and the organotin complexes

All the organotin complexes (**1-5**) were obtained as white/faint-yellow, air stable and crystalline solids with melting points ranging from 121 - 192 °C.

3.2 Infrared spectroscopy

The IR spectra obtained for the organotin(IV) dithiocarbamate complexes, offered useful information about the coordination mode and structure of the dithiocarbamate. The assignment of the spectral bands was carried out based on established peaks of similar structures in literature [32,33]. The C-N vibration of the thioureide band was observed in the range 1491 – 1482 cm^{-1} in each of the complexes. The coordination of the ligand to the organotin moieties resulted in the bands occurring at higher frequencies in the range associated with the double bond character of thiouride bond (N-CSS), due to the delocalization of electrons towards the central Sn metal [34]. The vibration frequency of C-N in the spectral of the complexes with a chloride ion within their molecule possesses slightly higher frequencies than their alky/aryl counterparts due to the electron withdrawing abilities of the chloride ion which increases the positive charge on nitrogen atom in the thioureide bond [35,36]. The C-S vibration bands in the organotin complexes were observed as a single peak in the region 960 – 1010 cm^{-1} in complexes 3, 4 and 5, which may suggest a bidentate mode; but as a splitted peak in this region for complexes 1 and 2 indicating an anisodentate coordination [35]. The vibrational bands in the region 448 – 403 cm^{-1} in the spectra of all the complexes were attributed to the presence of Sn-S, thus signifying the coordination of the sulfur atoms of the dithiocarbamate ligands to the tin metal center of the organotin moiety [32].

3.3 Nuclear magnetic resonance

The ^1H NMR of the complexes gave two major signals in the range 3.68 – 3.52 (singlet) for the methyl group and 7.42 – 7.11 ppm (multiplet) due to aromatic protons of the phenyl groups in the ligand moiety [37]. The signal of the protons of the CH_3 group attached to the Sn center in complex 3 was observed as a singlet at 1.51 ppm. The chemical shifts for the protons of the butyl

groups in complex 1 and 4 were observed in the range 2.38 – 0.95 ppm. This variation in the peak values along the chain was due to the shielding of protons of the butyl group attached to the Sn metal center which weakens along the carbon chain through the carbon nuclei [38]. The aromatic protons of the phenyl groups of the organotin moiety resonated in the range 7.99-7.52 ppm for complex 2 and 5.

The ^{13}C NMR spectra of the complexes showed signals due to the carbon atoms of the ligand moiety in the range 205.29 – 200.03 ppm and 50.01 – 46.46 ppm, which are attributed to the quaternary carbon ($-\text{CS}_2$) and the $-\text{CH}_3$ group attached to the nitrogen atom respectively. The somewhat downfield shift of the signals of the thiouride bond is due to electron distribution over the bond existing in the $-\text{CNS}_2\text{Sn}$ region. The high signal value of the carbon atom of the CH_3 group has been attributed to its bonding to the electron rich nitrogen. The signals for the carbon atoms of the phenyl moiety resonated between 147.33 and 125.76 ppm in all the complexes. Carbon signals of the methyl group in the organotin moiety resonated around 14.04 ppm in complex 3, in the range 33.39 – 13.86 ppm for the butyl group in complexes 1 and 4, and between 135.08 and 122.12 ppm for the phenyl group in complexes 2 and 5.

In the spectra of the ^{119}Sn NMR, the following chemical shift ranges: $\delta = 200$ to -60 , -90 to -190 and -210 to -400 ppm have been established for the tetra-, penta-, or hexa-coordinated organotin complexes respectively [39]. These ranges are dependent on factors such as electronegativity of the ligand, temperature and concentration employed in the experiment. The ^{119}Sn NMR chemical shifts indicated an octahedral geometry around the Sn metal.

3.4 X-ray crystallography

Information about the crystal structures and refinement parameters are summarized in Table 1. Useful bond angles and lengths needed for the description and prediction of the geometry are presented in Tables 2 and 3. The ORTEP plot for the complexes showing the structure and numbering of the complexes is shown in Figures 2 and 4, while the crystal packing of the complexes are shown in Figure 3 and 5.

3.4.1 Structural description of complex $(\text{CH}_3)_2\text{SnL}_2$ (3)

Complex 3 is monomeric possessing four molecules per unit cell as shown in the packing diagram in Figure 3. The four sulfur atoms of the ligands bonded to the central metal Sn atom in a bidentate chelating fashion resulting in a six coordinate geometry around the Sn center as shown in Figure 2. The Sn-S bond distances are Sn1-S11 [2.5199(7)], Sn1-S12 [2.9785(6)], Sn1-S21 [2.5259(5)] and Sn1-S22 [2.9479(7)]. The observed Sn-S bond distances showed that Sn1-S12 and Sn1-S22 are longer than the Sn1-S11 and Sn1-S21, hence resulting into an asymmetric molecule [40] with bonds which are anisobidentate in nature [41]. This anisobidentate bond is also a result of the slight opening of the C-Sn-C bond angle (142.06) towards 180° moving away from 109° . If/when the C-Sn-C bond angle becomes linear the nature of the bond becomes isobidentate [42]. The stronger Sn-S bonds have shorter bond distances with an acute angle cis to each other, and subtending at $83.80(2)$, while the longer Sn-S bonds are weak bonds possessing a bond angle of $146.16(2)$ which is less from being co-linear with each other [33]. Both type of Sn-S bonds (the longer and the shorter) from the observed interatomic distances are longer than the expected sum of the covalent radii of a typical Sn-S bonds (2.42 Å) but well below the expected van der Waals radii (3.97 Å) [43]. The increase coordination around the Sn atom resulted in a significant change from the bite angle of the chelating dithiocarbamate

ligand which in turn results in the different bond distances observed [43]. The observed C-S bond distances (S11-C11 [1.7419(16)], S12-C11 [1.6861(16)], S21-C21 [1.7432(16)], S22-C21 [1.6876(16)]) with an average value of 1.7147 (16) is shorter compared to a typical C-S bond (1.81 Å). This is indicative of a partial double bond character of the C-S bond usually associated with the dithiocarbamate ligands [44]. The bond between Sn and the attached methyl groups also significantly contribute to the observed distortion in the octahedral geometry for the complex. These -CH₃ groups (C3-Sn1-C4) are attached to the tin axially with a bond angle of 142.06(8) showing a deviation from a cis-trans pathway of the C-Sn-C bond which is expected at 134° [43]. The interatomic bond angles of the Sn-C bond observed from Table 2 show the association between the Sn-C bonds and the Sn-S bond. The bond angles S12-Sn1-C3 [83.40(60)], S12-Sn1-C4 [84.79(5)], S22-Sn1-C3 [86.12(6)], S22-Sn1-C4 [83.99(5)] reveals the bending of the Sn-C bonds towards the Sn-S bond with a higher distance. This was attributed to electronic (repulsion in the metal center and the bonding electron pair of the S atoms) and steric reasons [45]. The expected octahedral geometry observed due to the six coordination is distorted around the tin center atom due to unequal bond distances and the asymmetric nature of the dithiocarbamate ligands. Hence, this geometry is described as skew trapezoidal-bipyramidal [34].

3.4.2 Structural description of complex (C₄H₉)₂SnL₂ (4)

Complex 4 is triclinic with two molecules per unit cell as shown in the crystal packing diagram presented in Figure 5. The structure from the ORTEP plot in Figure 4 shows the coordination of dithiocarbamate ligands through sulfur atoms to the metal center in a monodentate fashion at the adjacent sides of the complex. The Sn-S bond distances observed are Sn1-S11 [2.5179(8)], Sn1-S12 [3.0275(8)], Sn1-S21 [2.507(7)] and Sn1-S22 [3.0465(9)]. These distances are similar

to complex 3, and results in the complex being asymmetrical. The longer bond can be regarded as a real bond because it falls significantly below the sum of the van der Waals radii (3.97 Å) [43]. The strong steric interaction of the two bulky butyl moieties attached to the Sn center might be responsible for this weak bond because it reduces the propensity for the coordination of the second pendant S atom [46]. The bulky size of the alkyl substituent and the phenyl ring may also play a role in preventing the Sn-S formation. These longer/weaker bonds create an anisobidentate mode of binding instead of a bidentate mode of binding with the Sn center and are less from being co-linear, possessing a bond angle of 148.29(2)° cis to each other. This anisobidentate bonding is also supported by the slight opening of the C-Sn-C bond angle (137.7°). The stronger Sn-S bonds are those with shorter bond distances with an acute angle cis to each other subtending at 83.10(2)° [33]. The bite angles of the sulfur atoms to the tin center result in a very significant distortion away from the expected octahedral geometry. The average value of the C-S bond (in Table 4) was 1.715 (3) Å which is shorter compared to a typical C-S bond (1.81 Å). This shows the partial double bond character often attributed to the dithiocarbamate complexes [44]. The C-Sn-C bond which is expected at 134° for the alkyl (C31-Sn1-C41) groups attached to the tin center was found axially at 137.7(6)°, showing a slight deviation from the cis-trans pathway of this bond [43]. The bond angles S12-Sn1-C31 [83.13(7)°], S12-Sn1-C41 [87.4(5)°], S22-Sn1-C31 [82.69(7)°], S22-Sn1-C41 [84.30(7)°] reveals the bending of the Sn-C bonds towards the Sn-S bond with a longer distance which is probably due to the bulkiness of this alkyl substituent. The distortion observed in this complex has been attributed to the several bonds around the tin metal which, in turn, resulted in changes in the interatomic distances and angles [44]. Therefore, the geometry around the Sn atom in this complex $(C_4H_9)_2SnL_2$ is best

described as distorted skew trapezoidal-bipyramidal, owing to the closeness of the double bonded sulfur atom, and this is similar to other reports Dibutyltin complex [34,46].

3.5 Thermogravimetric Analysis (TGA)

The Thermogravimetric and differential thermogravimetric (TG/DTG) curves carried out under nitrogen for the complexes show two types of decomposition patterns as shown in Figures 6 – 10 and the data obtained from the curves are summarized in Table 3. The DTG curves for complex 4 and 5 showed melting temperatures at 129 and 187 °C respectively, as observed in Figures 8 and 9. The decomposition of complexes 1, 2, 4 and 5 occurred in the temperature range of 98 – 144, 77 – 161, 160 – 399 and 116 – 192 °C respectively, resulting in a mass loss which agrees with the estimated loss of the -CH₃ attached to the N atom of the ligand moiety. The mass loss was found to be about 3.30, 2.50, 2.50 and 2.56% of the respective starting masses of complexes 1, 2, 4, and 5, which is close to the calculated values of 2.72, 2.50, 2.50, and 2.36%, respectively. The final decompositions step for the complexes occurred around 193 – 290, 203 – 427, 206 – 373, 249 – 325 °C respectively, for complexes 1, 2, 4, and 5, leaving residues which were about 25.03, 25.70, 23.90 and 22.18% of the respective starting masses. These were attributed SnS, whose expected mass (complex 1: 24.84; (2): 25.70; (4): 23.90 and (5) 23.46%) agreed with the calculated value of the residue in each case. In complex 3, the decomposition occurred as a single step in the temperature range of 160 – 399 °C to give a residue which was 28.8% of the starting mass attributed to SnS. This was found to be in agreement with the estimated theoretical mass of 28.8%.

The TGA showed that all the complexes gave tin sulfide as a final residue after their respective decomposition, hence indicating the potential of the complexes as precursors to SnS

nanoparticles. The different thermal decomposition pattern observed in complex 3 further confirms the dissimilarities in the decomposition pathways for structurally related organotin complexes [47].

3.6 Antimicrobial studies

The synthesized complexes 1 – 5 were screened *in vitro* for their antimicrobial activity against five bacterial organisms (*S. Aureus*, *B. cerues*, *K. pneumonia*, *P. aeruginosa* and *E. coli*) and two fungi organisms (*C. albican* and *A. flavus*) at three concentrations of 10, 25 and 50 $\mu\text{g/mL}$. Significant antimicrobial activity (inhibitory zone $>6\text{mm}$) was observed at 50 $\mu\text{g/mL}$, and the results obtained were taken as a measure of the antimicrobial potentials and minimum inhibitory concentration (MIC) of the complexes. The obtained data are presented in Table 5, and summarized as histogram in Figure 11. The results show that the bacterial organisms were more susceptible to the organotin complexes compared to the fungi organisms. Complex 5 gave the best antibacterial activity of the organotin complexes with inhibitory zone in the range of 10-21 mm. The least antibacterial results were obtained from complex 3, with inhibitory zone in the range of 8-15 mm. The pattern of the antibacterial results obtained for the complexes suggest that the Gram negative bacterial organisms were more susceptible to the complexes compared to the Gram positive organisms. This could be attributed to the structural difference between the two bacterial organisms. The Gram positive bacteria possess cell wall. The complexity of the cell wall is due to an outer-lipid membrane formed from lipopolysaccharide contributing to the antigenic specificity which does not permit easy penetration of the complexes into the bacteria [48–51]. The Gram negative bacterial organisms do not have cell walls but a simpler cell membrane that lacks the rigidity of the cell wall. Hence, they are more susceptible to the

complexes compared to the Gram positive bacterial organisms. It was also observed that complex 2 and 5 (with phenyl substituent) displayed better antibacterial activity compared to complex 1 and 4 (with butyl substituent) and complex 3 (with methyl substituent). This could be attributed to the increase in lipophilicity properties of the complexes through the lipid bilayer of the bacteria organisms due to the presence of the planar phenyl groups attached to the tin center [45].

The organotin complexes gave moderate antifungal activity with inhibitory zones in the range of 9-11 mm. The complex 2 showed the best antifungal activity compared to the other complexes. The positive control drugs gave better antimicrobial activity compared to the complexes. However, the antibacterial results of the complexes were in some cases comparable. The antimicrobial activity was assessed by measuring the inhibition halo of microbial growth around the well, and the results were classified according to the following scale: inhibition zones down to 9 mm, inactive; 9–12 mm, moderately active; 13–18 mm, active; above 18 mm, very active [52, 53]. Based on the scale, the complexes were moderately active against the fungi organisms but showed antibacterial activities ranging from moderately active to very active. Complex 5 was very active against the *P.aeruginosa*, *K.pneumonia* and *E.coli*.

Conclusion

Five new organotin(IV) derivatives of *N*-methyl-*N*-phenyldithiocarbamate (L) have been successfully synthesized and characterized. The single crystal X-ray analysis of complexes 3 and 4 indicated a six-coordinate geometry with a strong distortion around the tin center, which is ascribed to electronic and steric reasons. The asymmetric nature of the dithiocarbamate ligand

attached to the adjacent sides of the complexes resulted in skew-trapezoidal bipyramidal geometry. The thermal analysis showed closely related decomposition pattern except for complex 3. However, the final product of the decomposition for all the complexes was SnS indicating their usefulness as a single source precursor in materials chemistry. The organotin complexes exhibited good to moderate antimicrobial properties against some microbial organisms. However, the bacteria were more susceptible to the complexes compared to the fungi organisms.

Supplementary data

Crystallographic data of the complexes have been deposited with the Cambridge Crystallographic Data Center allocated with the deposit number CCDC 1551583 and 1551584. Copy of the data can be obtained free of charge on application to CCDC, 12 Union Road, Cambridge CB2 1EZ, UK, fax: +44 1223 336033, email:deposit@ccdc.cam.ac.uk.

References

- [1] R. Jain, R. Singh, N.K. Kaushik, *J. Chem.* 2013 (2013) 1.
- [2] S.S.A. Shah, M. Ashfaq, A. Waseem, M.M. Ahmed, T. Najam, S.S. and G. Rivera, *Mini-Reviews Med. Chem.* 15 (2015) 406.
- [3] H. Iqbal, S. Ali, S. Shahzadi, *Cogent Chem.* 1 (2015) 1029039.
- [4] M. Nath, *Appl. Organomet. Chem.* 22 (2008) 598.
- [5] T. Sedaghat, Z. Shokohi-Pour, *J. Coord. Chem.* 62 (2009) 3837.
- [6] G.A. Ayoko, J.J. Bonire, S.S. Abdulkadir, P.F. Olurinola, J.O. Ehinmidu, S. Kokot, S.

- Yiasel, *Appl. Organomet. Chem.* 17 (2003) 749.
- [7] M. Nath, S. Pokharia, G. Eng, X. Song, A. Kumar, *J. Organomet. Chem.* 669 (2003) 109.
- [8] M. Nath, S. Pokharia, X. Song, G. Eng, M. Gielen, M. Kemmer, M. Biesemans, R. Willem, D. De Vos, *Appl. Organomet. Chem.* 17 (2003) 305.
- [9] J. Susperregui, M. Bayle, G. Lain, C. Giroud, T. Baltz, *Eur. J. Med. Chem.* 34 (1999) 617.
- [10] M. Nath, R. Yadav, G. Eng, T. Nguyen, A. Kumar, *J. Organomet. Chem.* 577 (1999) 1.
- [11] D. Kovala-Demertzi, V. Dokorou, Z. Ciunik, N. Kourkoumelis, M.A. Demertzis, *Appl. Organomet. Chem.* 16 (2002) 360.
- [12] M. Nath, S. Pokharia, R. Yadav, *Coord. Chem. Rev.* 215 (2001) 99.
- [13] S. Shahzadi, S. Ali, *J. Iran. Chem. Soc.* 5 (2008) 16.
- [14] A.C. Ekennia, D.C. Onwudiwe, A.A. Osowole, *J. Sulfur Chem.* 36 (2015) 96.
- [15] T. Sedaghat, K. Goodarzi, *Main Gr. Chem.* 4 (2005) 121.
- [16] J.J. Criado, J.A. Lopez-Arias, B. Macias, L.R. Fernandez-Lago, J.M. Salas, *Inorganica Chim. Acta.* 193 (1992) 229.
- [17] J.J. Criado, A. Carrasco, B. Macias, J.M. Salas, M. Medarde, M. Castillo, *Inorganica Chim. Acta.* 160 (1989) 37.
- [18] R. Cao, N. Travieso, A. Fragoso, R. Villalonga, A. Diaz, M.E. Martinez, J. Alpizar, D.X. West, *J. Inorg. Biochem.* 66 (1997) 213.
- [19] L. Ji, B. Ye, H. Yang, T. Zeng, *J. Inorg. Biochem.* 51 (1993) 428.
- [20] N. Awang, N.F. Kamaludin, I. Baba, K.M. Chan, N.F. Rajab, A. Hamid, *Orient. J. Chem.* 32 (2016) 101.
- [21] T.S.B. Baul, *Appl. Organomet. Chem.* 22 (2008) 195.
- [22] M. Jabeen, S. Ali, S. Shahzadi, M. Shahid, Q.M. Khan, S.K. Sharma, K. Qanungo, *J. Iran.*

- Chem. Soc. 9 (2012) 307.
- [23] A.C. Ekennia, D.C. Onwudiwe, C. Ume, E.E. Ebenso, *Bioinorg. Chem. Appl.* 2015 (2015).
- [24] Bruker, APEX2, SAINT, SADABS. Bruker AXS Inc., Madison, Wisconsin, USA. (2007).
- [25] G.M. Sheldrick, Crystal structure refinement with SHELXL, *Acta Crystallogr. Sect. C Struct. Chem.* 71 (2015) 3.
- [26] G.M. Sheldrick, SHELXT - Integrated space-group and crystal-structure determination, *Acta Crystallogr. Sect. A Found. Crystallogr.* 71 (2015) 3.
- [27] G.M. Sheldrick, A short history of SHELX, *Acta Crystallogr. Sect. A Found. Crystallogr.* 64 (2007) 112.
- [28] W.P.. Ross, P.W. and Malbrook, *Clinical and oral microbiology*, Hemisphere Publishing Corporation, New York, 1982.
- [29] M. Balouiri, M. Sadiki, S.K. Ibnsouda, *J. Pharm. Anal.* 6 (2016) 71.
- [30] B. Fernández-torres, I. Inza, J. Guarro, *Antimicrob. Agents Chemother.* 49 (2005) 2116.
- [31] H.J. Simon, E.J. Yin, *Appl. Envir. Microbiol.* 19 (1970) 573.
- [32] J.P. Fuentes-Martínez, I. Toledo-Martínez, P. Román-Bravo, P.G. y. García, C. Godoy-Alcántar, M. López-Cardoso, H. Morales-Rojas, *Polyhedron.* 28 (2009) 3953.
- [33] N. Singh, S. Bhattacharya, *J. Organomet. Chem.* 700 (2012) 69.
- [34] Zia-ur-Rehman, N. Muhammad, S. Ali, I.S. Butler, A. Meetsma, *Inorganica Chim. Acta.* 376 (2011) 381.
- [35] S. Ali, Zia-Ur-Rehman, Muneeb-Ur-Rehman, I. Khan, S.N.A. Shah, R.F. Ali, A. Shah, A. Badshah, K. Akbar, F. Bélanger-Gariepy, *J. Coord. Chem.* 67 (2014) 3414.
- [36] F. Bonati, R. Ugo, *J. Organomet. Chem.* 10 (1967) 257.

- [37] M.K. Gupta, H.L. Singh, S. Varshney, A.K. Varshney, *Bioinorg. Chem. Appl.* 1 (2003) 309.
- [38] N. Khan, Y. Farina, L.K. Mun, N.F. Rajab, N. Awang, *Polyhedron*. 85 (2015) 754.
- [39] M. Sirajuddin, S. Ali, M.N. Tahir, *Inorg. Chim. Acta.* 439 (2016) 145.
- [40] R. Yadav, M. Trivedi, R. Chauhan, R. Prasad, G. Kociok-Köhn, A. Kumar, *Inorganica Chim. Acta.* 450 (2016) 57.
- [41] J. S. Morris; E. O. Schlemper, *J. Cryst. Mol. Struct.* 8 (1979) 295.
- [42] P.A. Cusack, *Chemistry of Tin*, 2nd Edition, Blackie Academic and professional, London, 1997.
- [43] R. Yadav, M. Trivedi, R. Chauhan, R. Prasad, G. Kociok-Köhn, A. Kumar, *Inorganica Chim. Acta.* 450 (2016) 57.
- [44] D.C. Onwudiwe, P.A. Ajibade, B. Omondi, *J. Mol. Struct.* 987 (2011) 58.
- [45] F. Shaheen, Zia-Ur-Rehman, S. Ali, A. Meetsma, *Polyhedron*. 31 (2012) 697.
- [46] N. Awang, I. Baba, N.S.A. Mohd Yousof, N.F. Kamaludin, *Am. J. Appl. Sci.* 7 (2010) 1047.
- [47] J.O. Hill, S. Chirawongaram, *J. Therm. Anal.* 41 (1994) 511.
- [48] A.C. Ekennia, D.C. Onwudiwe, A.A. Osowole, L.O. Olasunkanmi, E.E. Ebenso, *J. Chem.* 2016 (2016) 1.
- [49] S. Jabbar, I. Shahzadi, R. Rehman, H. Iqbal, Qurat-Ul-Ain, A. Jamil, R. Kousar, S. Ali, S. Shahzadi, M.A. Choudhary, M. Shahid, Q.M. Khan, S.K. Sharma, K. Qanungo, *J. Coord. Chem.* 65 (2012) 572.
- [50] Y. Anjaneyulu, R.P. Rao, *Synth. React. Inorg. Met. Chem.* 16 (1986) 257.
- [51] F. Javed, M. Sirajuddin, S. Ali, N. Khalid, M.N. Tahir, N.A. Shah, Z. Rasheed, M.R.

Khan, Polyhedron. 104 (2016) 80.

[52] T.M.A. Alves, A.F. Silva, M. Brandão, T.S. Grandi, E. Smânia, A. Smânia Júnior, C.L.

Zani. Memórias do Instituto Oswaldo Cruz. 95(2000)367.

[53] A. C. O. Silva, E. F. Santana, A.M. Saraiva, F. N. Coutinho, R. H. A. Castro, M. N. C. Pisciotano, E. L.C. Amorim and U. P. Albuquerque. Evid Based Complement Alternat Med. (2013). Doi: 10.1155/2013/308980.

ACCEPTED MANUSCRIPT

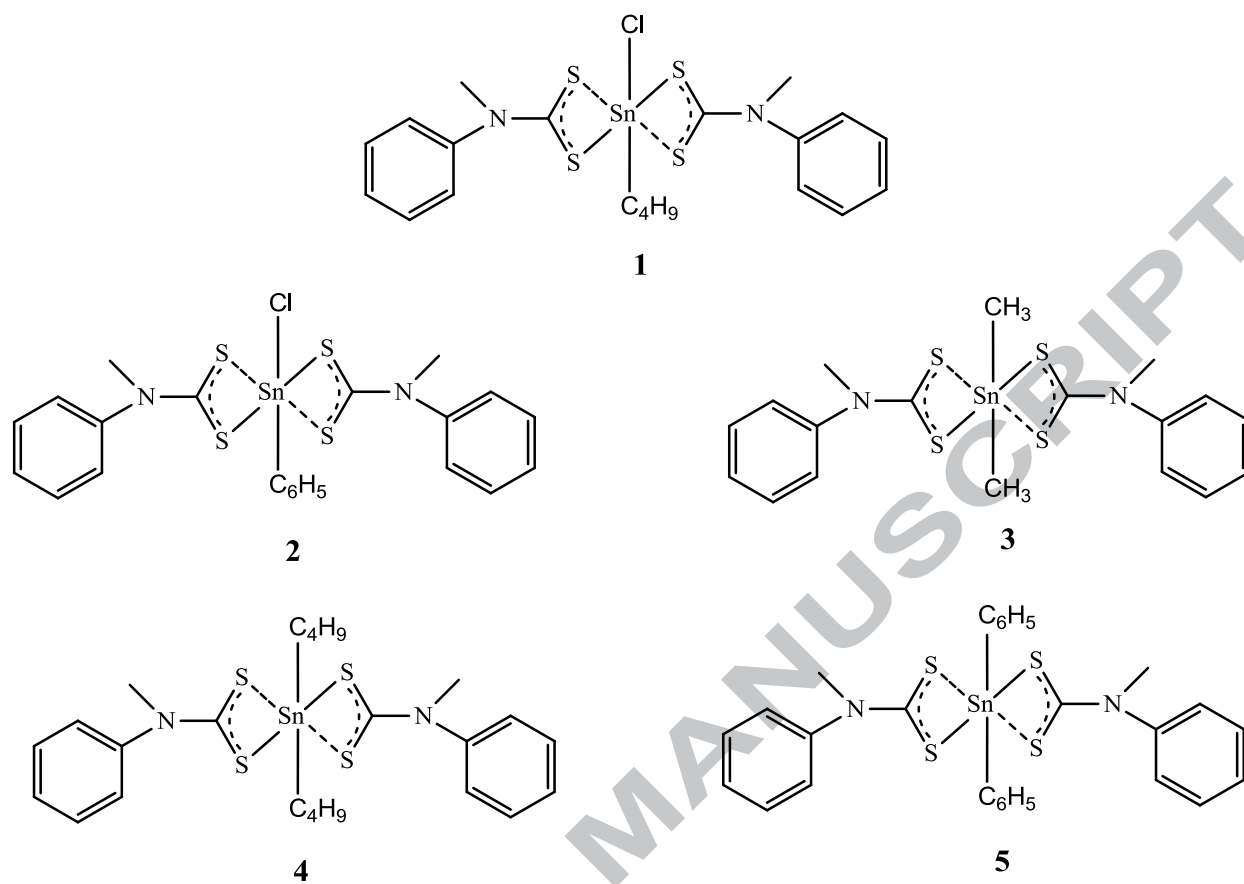


Figure 1: Structure of the organotin(IV) complexes

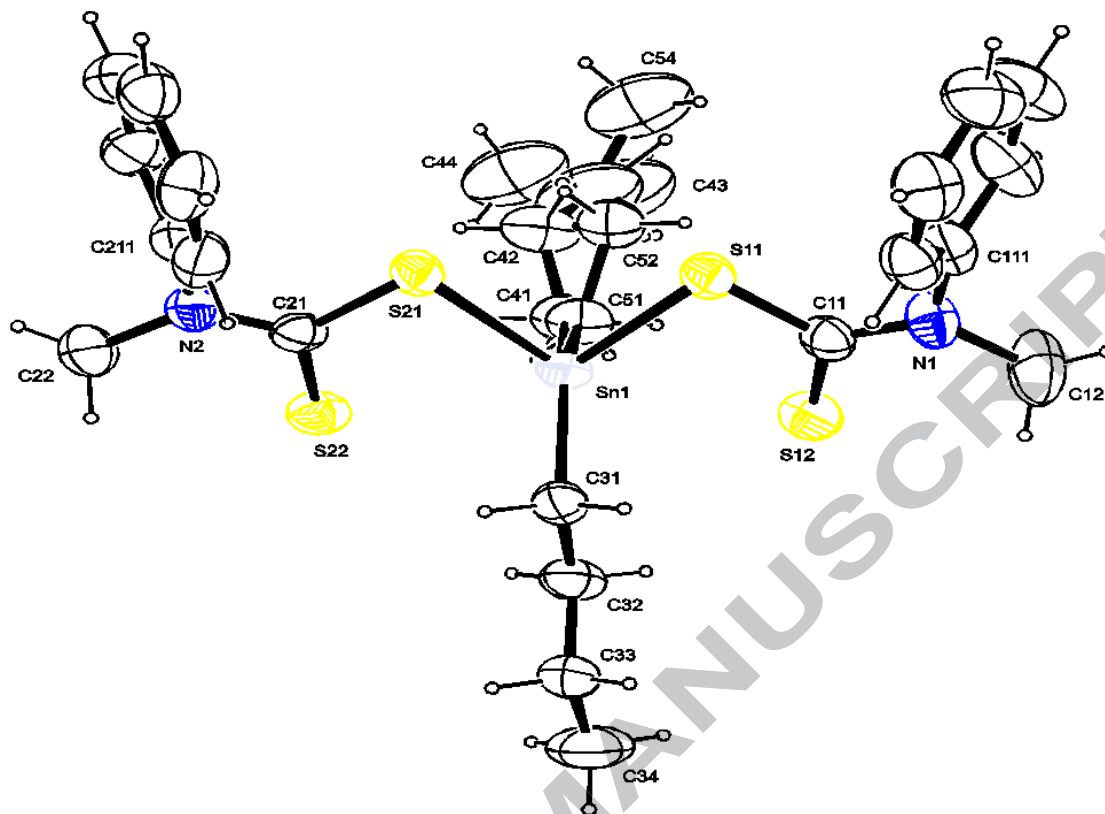


Figure 4: Structure of 4 drawn at 50% probability level displacement ellipsoids.

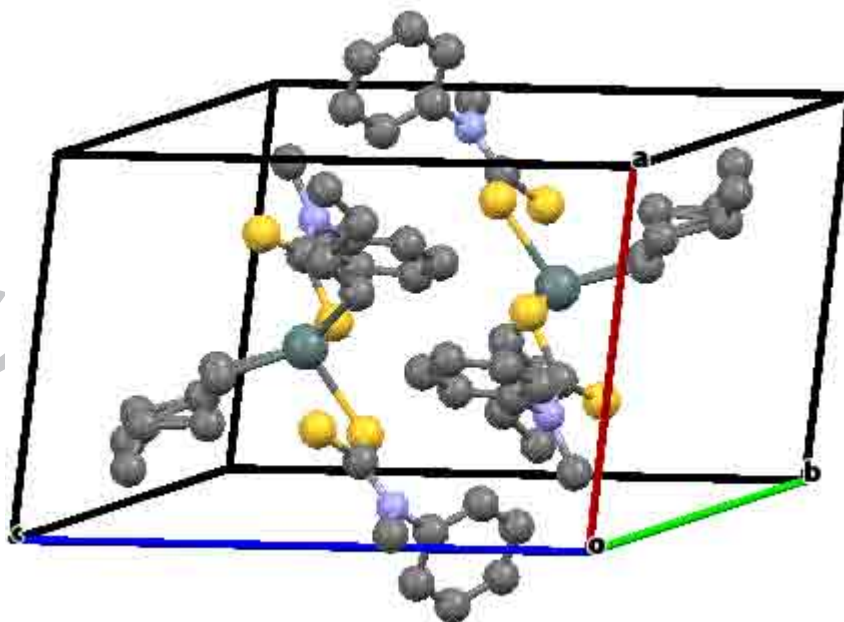


Figure 5: Crystal packing of 4 viewed along the best axis (hydrogen atoms removed for clarity).

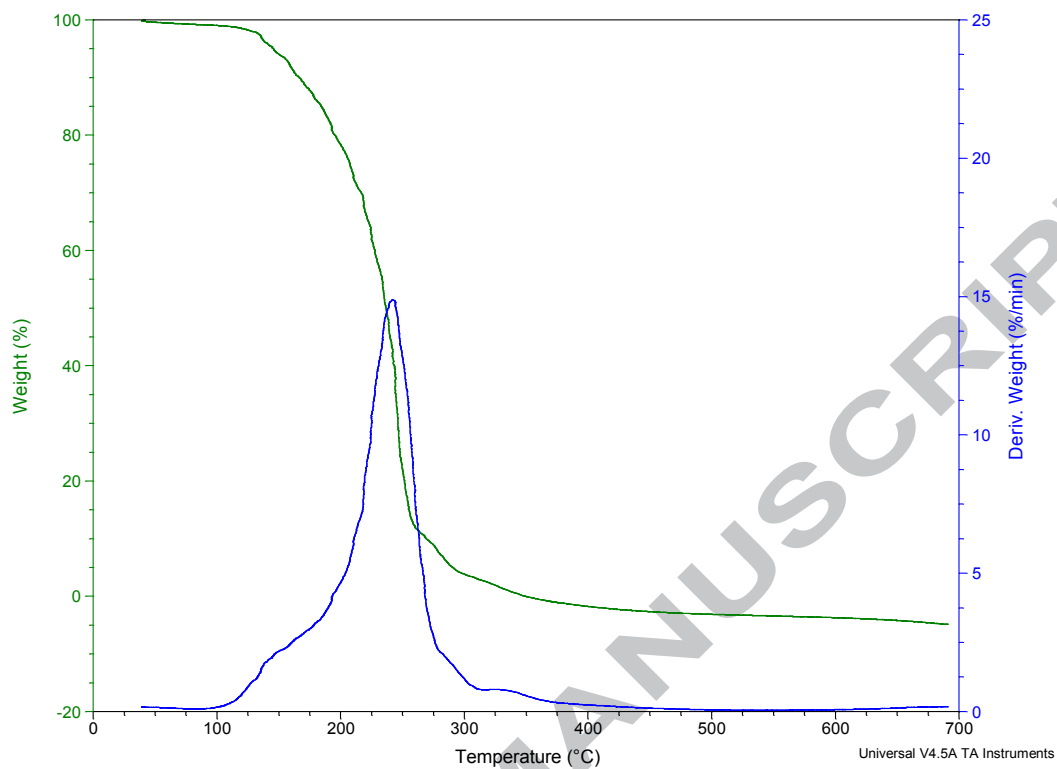


Figure 6. TG and DTG curves (with heating rate 10 °C/min) of complex 1 in N₂ atmosphere (75 mL/ min)

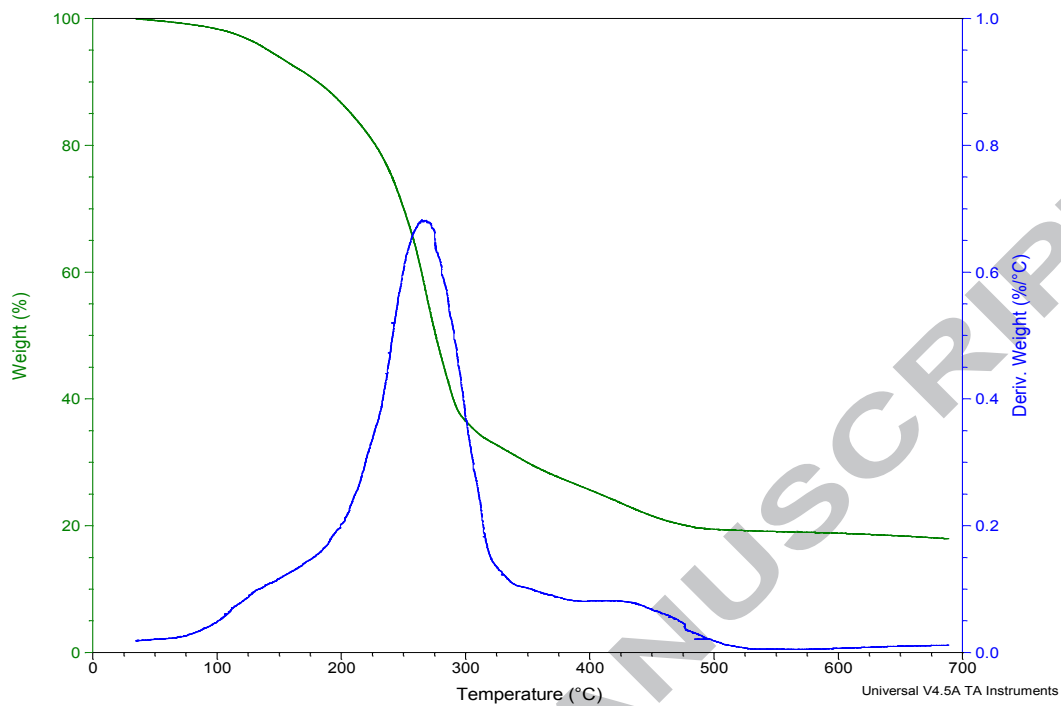


Figure 7. TG and DTG curves (with heating rate 10 °C/min) of complex 2 in N₂ atmosphere (75 mL/ min)

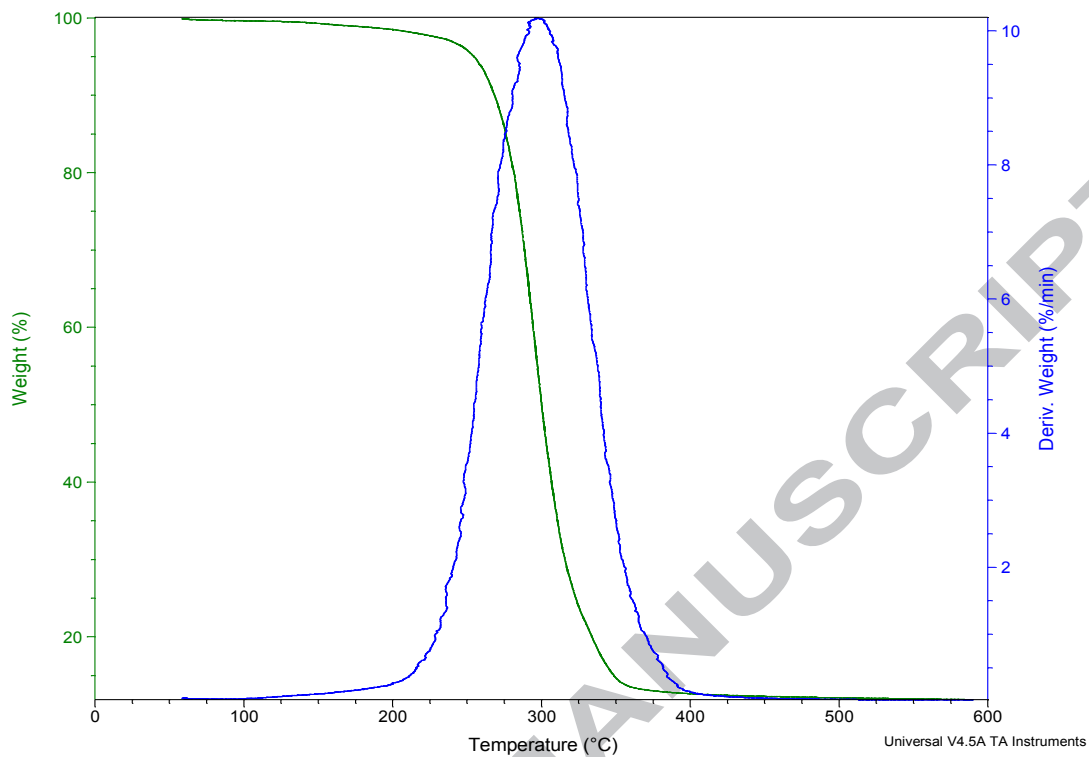


Figure 8. TG and DTG curves (with heating rate 10 °C/min) of complex 3 in N₂ atmosphere (75 mL/ min)

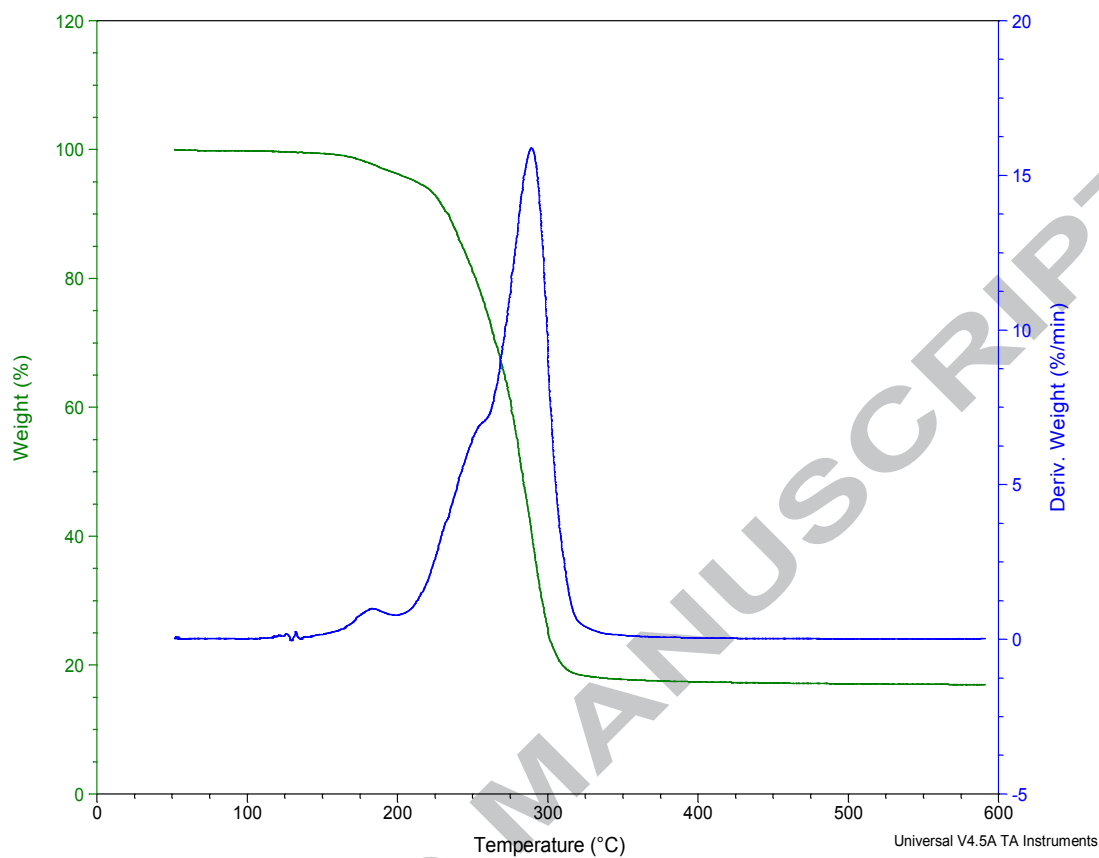


Figure 9. TG and DTG curves (with heating rate 10 °C/min) of complex 4 in N₂ atmosphere (75 mL/ min)

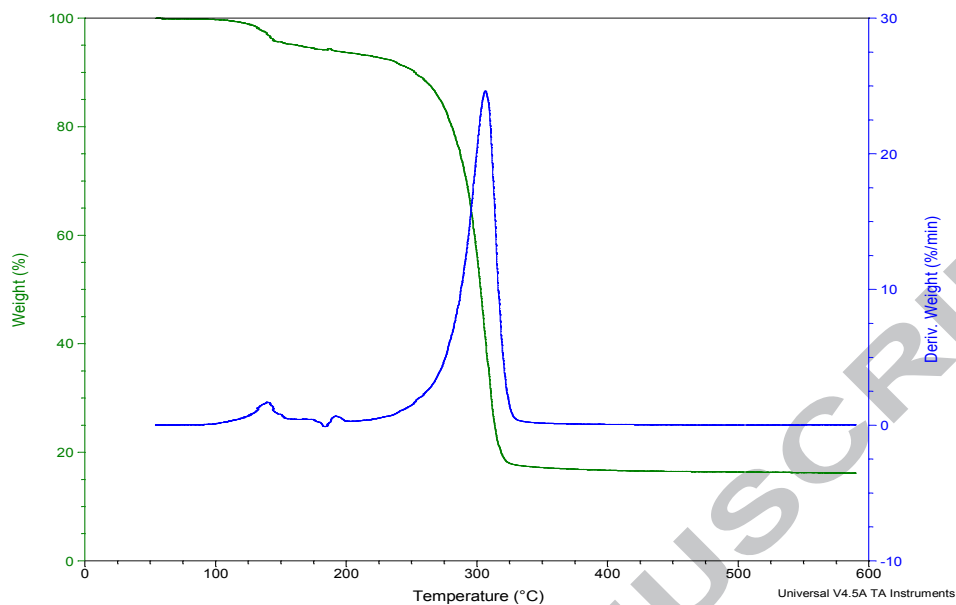


Figure 10. TG and DTG curves (with heating rate 10 °C/min) of complex 5 in N₂ atmosphere (75 mL/ min)

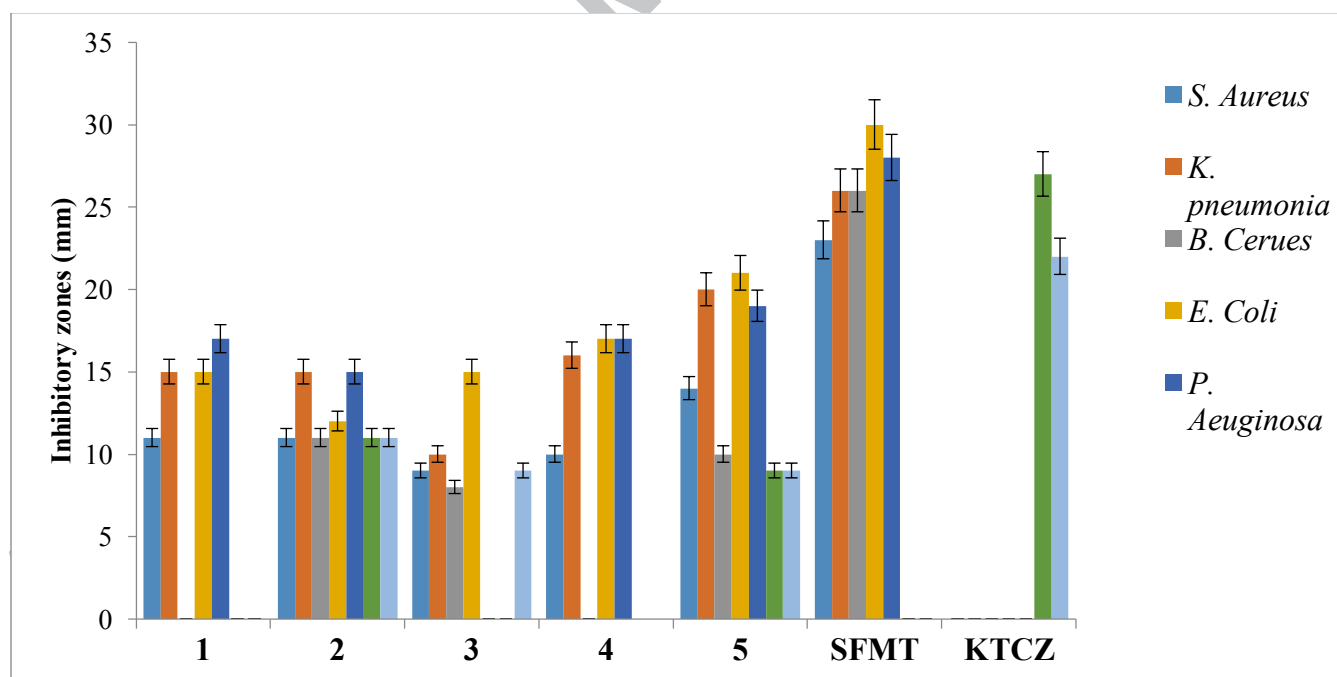


Figure 11: Histogram showing antimicrobial activity of complex 1- 5

Table 1: Crystallographic data and refinement parameters for complex $(\text{CH}_3)_2\text{SnL}_2$ and $(\text{C}_4\text{H}_9)_2\text{SnL}_2$

Parameters	$(\text{CH}_3)_2\text{SnL}_2$ (3)	$(\text{C}_4\text{H}_9)_2\text{SnL}_2$ (4)
Empirical formula	$\text{C}_{18}\text{H}_{22}\text{N}_2\text{S}_4\text{Sn}$	$\text{C}_{24}\text{H}_{34}\text{N}_2\text{S}_4\text{Sn}$
Formula weight	513.33	597.48
Crystal size (mm)	0.22 x 0.34 x 0.52	0.22 x 0.34 x 0.52
Crystal system	monoclinic	triclinic
Crystal habit	colorless needle	colorless needle
Space group	P21/c (No. 14)	P-1(No. 2)
a (Å)	11.1556(6)	10.9795(5)
b (Å)	7.7350(4)	11.8505(5)
c (Å)	25.9770(12)	13.4456(6)
β (°)	96.257(2)	94.122(2)
U (Å ³)	2228.2(2)	1424.39(12)
Z	4	2
D_{calc} (g cm ⁻³)	1.530	1.393
$F(000)$	1032	612
θ range (°)	1.8 - 28.3	1.7 - 28.3
Index range	-14:14;-10:9;-33:34	-14:14;-15:15;-17: 17
Total, unique reflections	91346,5549,	48933,7058
Observed reflections $I > 2\sigma(I)$	5128	6130
Number of parameters refined	230	296
Final R , $wR2$	0.0186, 0.0441	0.0279, 0.0740
Goodness-of-fit (GOF)	0.00	0.00

Table 2: Selected interatomic distances and angles for $(\text{CH}_3)_2\text{SnL}_2$

$(\text{CH}_3)_2\text{SnL}_2$	
Bond distances (Å)	
Sn1-S11	2.5199(7)
Sn1-S12	2.9785(6)
Sn1-S21	2.5259(5)
Sn1-S22	2.9479(7)
Sn1-C3	2.121(2)
Sn1-C4	2.1193(17)
S11-C11	1.7419(16)
S12-C11	1.6861(16)
S21-C21	1.7432(16)
S22-C21	1.6876(16)
N1-C11	1.337(2)
N1-C12	1.466(2)
N1-C111	1.444(2)
N2-C21	1.335(2)
N2-C22	1.470(2)
N2-C211	1.440(2)
Bond angles (°)	
S11-Sn1-S12	65.11(2)
S11-Sn1-S21	83.80(2)
S11-Sn1-S22	148.62(2)
S11-Sn1-C3	105.71(6)
S11-Sn1-C4	101.61(5)
S12-Sn1-S21	148.49(2)
S12-Sn1-S22	146.16(2)
S12-Sn1-C3	83.40(6)
S12-Sn1-C4	84.79(5)
S21-Sn1-S22	65.24(2)
S21-Sn1-C3	101.16(6)
S21-Sn1-C4	107.56(6)
S22-Sn1-C3	86.12(6)

S22-Sn1-C4	83.99(5)
C3-Sn1-C4	142.06(8)
Sn1-S11-C11	93.80(5)
Sn1-S12-C11	79.97(5)
Sn1-S21-C21	93.65(6)
Sn1-S22-C21	80.99(6)
C11-N1-C12	121.45(14)
C11-N1-C111	121.13(13)
C12-N1-C111	117.27(13)
C21-N2-C22	121.42(15)
C21-N2-C211	121.01(13)
C22-N2-C211	117.49(14)
S11-C11-S12	121.03(9)
S11-C11-N1	116.90(11)
S12-C11-N1	122.06(12)
S21-C21-S22	120.05(9)
S21-C21-N2	117.51(12)
S22-C21-N2	122.42(12)

Symmetry element i: -X, 1/2+Y, 1/2-Z

Table 3: Selected interatomic distances and angles for $(\text{C}_4\text{H}_9)_2\text{SnL}_2$

$(\text{C}_4\text{H}_9)_2\text{SnL}_2$	
Bond distances (Å)	
Sn1-S11	2.5179(8)
Sn1-S12	3.0275(8)
Sn1-S21	2.5073(7)
Sn1-S22	3.0465(9)
Sn1-C31	2.137(2)
Sn1-C41	2.16(2)
S11-C11	1.741(2)
S12-C11	1.685(3)
S21-C21	1.745(3)
S22-C21	1.690(3)
N1-C11	1.339(4)
N1-C12	1.475(5)
N1-C111	1.449(4)
N2-C21	1.342(3)

N2-C22	1.465(4)
N2-C211	1.439(3)
Bond angles (°)	
S11-Sn1-S12	64.19(2)
S11-Sn1-S21	83.10(2)
S11-Sn1-S22	147.29(2)
S11-Sn1-C31	105.14(7)
S11-Sn1-C41	107.4(7)
S12-Sn1-S21	147.27(3)
S12-Sn1-S22	148.29(2)
S12-Sn1-C31	83.13(7)
S12-Sn1-C41	87.4(6)
S21-Sn1-S22	64.28(2)
S21-Sn1-C31	105.65(7)
S21-Sn1-C41	104.4(6)

S22-Sn1-C31	82.69(7)
S22-Sn1-C41	84.3(7)
C31-Sn1-C41	137.7(6)
Sn1-S11-C11	95.04(9)
Sn1-S12-C11	79.47(8)
Sn1-S21-C21	95.43(8)
Sn1-S22-C21	78.93(9)
C11-N1-C12	120.8(2)
C11-N1-C111	121.9(2)
C12-N1-C111	117.2(2)
C21-N2-C22	121.8(2)
C21-N2-C211	121.3(2)
C22-N2-C211	116.9(2)
S11-C11-S12	120.67(15)
S11-C11-N1	117.25(19)
S12-C11-N1	122.08(19)
S21-C21-S22	120.96(14)
S21-C21-N2	116.67(19)
S22-C21-N2	122.4(2)

Table 4: Thermal analysis data of the complexes

Compounds	1	2	3	4	5
Temp range of decomp. (°C)	98 – 143	77 – 161	160 – 399	116 – 192	108 – 154
First stage	193 – 290	203 – 427	—	206 - 373	249 – 325
Second stage			—		
DTG peak T(°C)	137	113	304	185	138
First stage	247	399			315
Second					

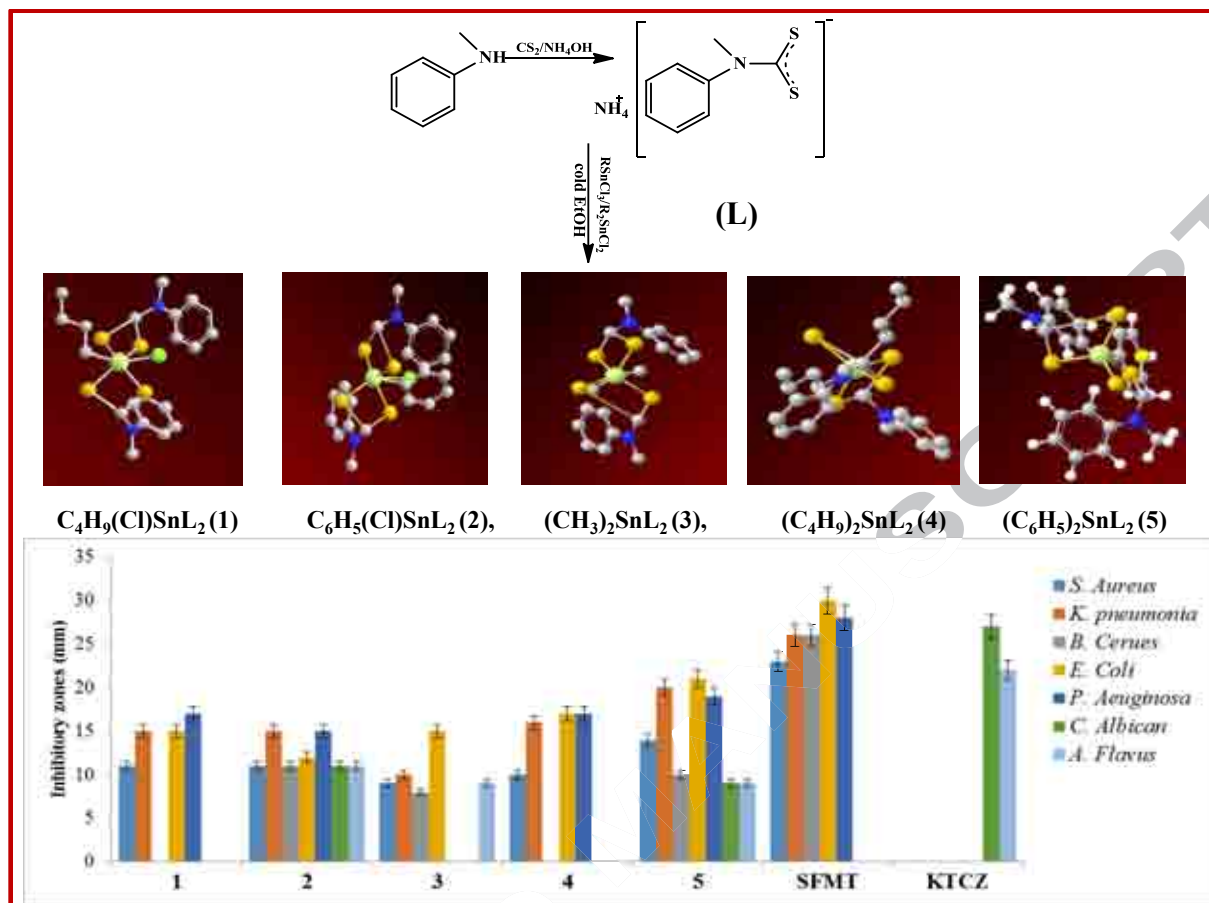
stage					
Melting point	————	————	———	129	186
Products Obtained	$[(C_6H_5)_2(CH_3)(CN)_2S_4]$	$[(C_6H_5)_2(CH_3)(CN)_2S_4]$	SnS	$[(C_6H_5)_2(CH_3)(CN)_2S_4]$	$[(C_6H_5)_2(CH_3)(CN)_2S_4]$
1 st decomposition	ClSn(C ₄ H ₉)	ClSn(C ₆ H ₅)	———	S ₄]Sn(C ₄ H ₉) ₂	S ₄]Sn(C ₆ H ₅) ₂
2 nd decomposition	SnS	SnS	———	SnS	SnS
Mass of residue (mg)					
Found	4.08 (4.18)	16.60 (16.)	3.16	16.00 (16.01)	9.07 (9.05)
(Calc)	1.10 (1.05)	4.37 (4.37)	(3.16)	4.00 (4.05)	2.06 (2.18)
First stage			———		
Second stage			———		

Compounds	Bacteria					Fungi	
	<i>S. aureus</i>	<i>K. pneumonia</i>	<i>B. cerues</i>	<i>E. coli</i>	<i>P. aeruginosa</i>	<i>C. albican</i>	<i>A. flavus</i>
1	11 ±0.7	15 ±0.7	-	15 ±1.4	17 ±1.4	-	-
2	11 ±0.7	15 ±0.7	11 ±0.0	12 ±2.1	15 ±0.7	11 ±0.7	11 ±2.1
3	09 ±1.4	10 ±0.0	08 ±0.0	15 ±0.0	-	-	09 ±0.7
4	10 ±0.7	16 ±0.7	-	17 ±2.1	17 ±0.7	-	-
5	14 ±2.1	20 ±0.0	10 ±0.0	21 ±1.4	19 ±0.7	09 ±2.1	09 ±2.1

Sulfamethoxazole (SFMT)	23 ±0.7	26 ±0.0	26 ±0.4	30 ±0.4	28 ±0.0	-	-
Ketoconazole (KTCZ)	-	-	-	-	-	27 ±0.7	22 ±0.7

Table 5: Summary of antimicrobial screening of complexes 1 - 5

50µg/ML (quadruplet results)



Highlights

- Organotin(IV)*N*-methyl-*N*-phenyldithiocarbamate complexes were synthesized and characterized.
- The methyl and butyl substituted complexes showed a distorted octahedral geometry.
- All complexes decomposed to tin sulfide, under inert atm.
- All the complexes showed potential as antimicrobial agents.
- The antimicrobial potency of the complexes is greater compared to their antifungal.